O 8. APPLICATION OF MAGNETIC BIOCHAR PRODUCED FROM ORANGE TREE SAWDUST AS AN ADSORBENT FOR THE REMOVAL OF CR (VI) IN WATERY ENVIRONMENT

Şerife Parlayıcı[1*], Kübra Tuna[1], Erol Pehlivan[1]

[1] *Konya Technical University, Chemical Engineering Department, Campus 42079 Konya, Turkey*

E-mail: serife842@hotmail.com, kubratnaa@gmail.com, erolpehlivan@gmail.com

ABSTRACT: In the present work, biochar was obtained from orange tree sawdust (OTS) and then it converted to magnetic form by a series treatment. This substance was applied as an ideal adsorbent for removal Cr (VI) from aqueous solution. The novel magnetic biochar (MB**ϖ**OTS) originated from OTS is likely to enhance the adsorption potential of Cr (VI). The adsorption of Cr (VI) by MB**ϖ**OTS and OTS was compared with each other for series of adsorption parameters. Magnetic form of OTS was constituted with $FeCl_3.6H_2O$ and $FeSO_4.7H_2O$ in a basic medium. The Magnetic OTS was heated in an oven at 500 ºC for 60 min. The produced magnetic char was applied for the removal of Cr (VI). The optimum conditions for the maximum Cr (VI) adsorption by MB**ϖ**OTS were determined as; 0.05 g adsorbent dosage, 40 mg/L Cr (VI) initial concentration, pH 2.01 and contact time, 180 min. The adsorption data were described well by the Langmuir isotherm model (R^2=0.985) compared to the Freundlich isotherm model (R^2=0.969). The maximum Cr (VI) adsorption capacity were calculated from the Langmuir equation was 30.36 mg/g for MB**ϖ**OTS and 11.75 mg/g for OTS. The adsorption capacity of MB**ϖ**OTS was higher than the capacity of raw OTS. The results showed that MB**ϖ**OTS can be an alternative adsorbent for the removal of Cr (VI) in the aquatic environment.

Keywords: Magnetic Biochar, Cr (VI), Adsorption, Kinetics

1. INTRODUCTION

Development industrial activities are highly threatening the clean water resources. Wastewaters are dumping from the industry without any treatment, so this situation causes a significant increase in chromium in soil, surface and groundwater resources (Vilardi et al. 2018). These kinds of wastewater contain heavy metal ions, which is a serious threat to both human health and all ecosystem. Heavy metals are non-biodegradable and have a tendency to accumulate in tissues through feeding and skin adsorption in all living tissues, from water microorganisms to animals and humans (Son et al. 2018). For example, if a certain concentration is exceeded in the body, it causes various diseases. Especially, chromium is widely used in many industrial applications. The wastewater released after various industrial activities sometimes contains trace amounts, sometimes-high concentrations of Cr (VI).

The most common wastewater containing chromium is released by paper, petrochemical, chlor-alkali production, fertilizer, iron and steel, leather and energy production (thermal) industries (Jia et al. 2018). Therefore, keeping the level of chromium in the wastewater at the limit level has been important in terms of environmental pollution. Regardless of its source, chromium pollution in drinking water is a serious problem in many parts of the world (Qian et al. 2019). The chromium exists either Cr (VI) or Cr (III) form in the environment. Cr (VI) is more toxic than Cr (III), which its analysis in environmental samples is more important. The removal of Cr (VI) ions from waters has been one of the most important issues investigated in the world (Lu et al. 2017). According to drinking water quality guidelines prescribed by the World Health Organization (WHO, 2011), the concentration of Cr (VI) in drinking water should not exceed 0.05 mg/L. It is important to control Cr (VI) pollution due to its toxicity. For this reason, the drinking water standards require an acceptable level of the metal ion in the medium and this requires new and highly effective treatment technologies (Zhang et al. 2019).

Numerous scientific researches and investigations have been carried out to determine and remove the levels of Cr (VI) ions causing pollution, and researchers have used a number of different analytical techniques and methods (Han et al. 2016; Shang et al. 2017). Generally, the methods used to treat wastewater containing heavy metal ions are chemical extraction (Yao et al. 2019), chemical oxidation-reduction (Huang et al. 2019), reverse osmosis (Gaikward et al. 2017), membrane separation (Laqbaqbia et al. 2019), ion exchange (Cao et al. 2018), adsorption (Cherdchoo et al. 2019) and biosorption (Xining

et al. 2015). One of the processes commonly used in the treatment of industrial wastewater is adsorption. The most significant advantage of adsorption based methods is the ability to separate trace amounts of pollutants from the large volume of wastewater. The adsorption method for heavy metals exist in the wastewater is a more economical and effective method compared to other separation methods depending on the type of adsorbent applied (Wang et al. 2014). For this reason, natural adsorbents are preferred in industrial applications and the related technologies are carried out on the development of adsorbents that can realize their adsorption activities more economically in wider application areas. Especially industrial and agricultural by-products are evaluated as adsorbents and solutions for current problems in the waste management area and lower cost adsorbents can be obtained. Appropriate assessment of these wastes and wastes is very important in preventing the national economy and environmental pollution (Chen et al. 2018).

OTS is abundant in nature and it is a low-price material. It can be used as a suitable adsorbent for the removal of toxic metals in wastewater in the present and modified form (Shukla et al. 2002). This material obtained as a by-product in wood production plants in the solid form and can be used as a low-cost adsorbent for the removal of heavy metals from water. OTS consist of (45-50%) cellulose and (23-30%) lignin, which contain hydroxyl, carboxylic and phenolic groups (Zakaria et al. 2009). The OTS can be treated with magnetic materials to increase the capacity of heavy metal bonding.

Biochar is a carbon-rich solid created by high-temperature pyrolysis of biomass heating in the absence of oxygen. Biochar has interested appreciable relevance in recent times owing to its remarkable properties, for example, its low cost, eco-friendliness, and the wide range of available feedstock materials, as well as mechanical and thermal stability, which facilitate the application of biochar in many environmental areas (Yap et al. 2017; Shang et al. 2017; Lyu et al. 2017). Furthermore, the feedstocks of biochar production can be acquired from a variety of waste biomass and produced at low cost, which mainly obtained from agricultural biomass and solid waste (Rajapaksha et al. 2018; Tan et al. 2015). Nowadays, the removal of heavy metals has become a key area of research interest in relation to the potential of biochar for wastewater remediation (Qian et al. 2019). As an adsorbent, MB**ϖ**OTS has a porous structure similar to activated carbon, which is the most commonly employed and efficient adsorbent for the removal of chromium from water throughout the World (Wei et al. 2018; Zhang et al. 2019). Moreover, MB**ϖ**OTS contains a large amount of oxygen-containing groups on the surface, which are quite effective for the adsorption of chromium. MB**ϖ**OTS has been found to provide effective adsorptivity, ready separation, and easy recycling. MB**ϖ**OTS described among these approaches and successfully produced by chemical co-precipitation of iron oxides. Recent studies have tended to use compounds or mixtures of biochar and iron-based materials to remediate pollutants (Qian et al. 2017). The recoverable magnetic biochar derived from orange tree sawdust is a good potential for water remediation (Shan et al. 2014).

In the present study, the main target is to produce MB**ϖ**OTS from OTS with much higher capacity and to try the different parameters related to adsorption of Cr (VI) from the solution phase onto the MB**ϖ**OTS. The parameters such as contact time, adsorbent dosage, initial metal ion concentration, and pH were investigated for the equilibrium stage. Applying the parameters obtained from the isotherm plot, the adsorbent capacities were determined.

2. MATERIALS AND METHODS

2.1. Materials

$FeCl_3.6H_2O$, $FeSO_4.7H_2O$, NH_4OH, NaOH and HCl solutions were obtained from Merck Company. The pH of solutions was adjusted by adding 0.1 M NaOH and HCl solution. Ultrapure water was used throughout this study for all cleaning procedures and the dilution of concentrated solutions. Cr (VI) solutions were prepared using $K_2Cr_2O_7$. Stock solution (1000 mg/L) of Cr (VI) was prepared by dissolving the required quantity of $K_2Cr_2O_7$ in ultrapure water.

For the adsorption experiments, Orion 900S2 Model pH meter, a thermo explicit shaker of GFL 3033 model was used for the simple adjustment of pH and mixing the solutions. UV-Visible Spectrophotometer (Shimadzu UV-1700) was used to determine the Cr (VI) concentration in all samples. The microstructure of the MBϖOTS was examined by using a scanning electron microscope (SEM, Nova Nano SEM 200, FEI Company). The samples were coated with a fine gold before the measurement and then sprayed at 20kV in SEM.

2.2. Preparation of the Adsorbents

OTS was prepared from the orange trees garden in the southern parts of Muğla-Turkey. They were trimmed and washed several times with pure water. The woodchip obtained in natural condition were meshed with a saw machine and then dried in the oven. After that, they sieved in certain mesh sizes (65-125 µm).

Magnetic orange tree sawdust MωOTS (Figure 1.) was synthesized by a simple chemical precipitation method. OTS (5 g), $FeCl_3.6H_2O$ (6 g) and $FeSO_4.7H_2O$ (4 g) were transferred into a flask containing 100 mL of pure water. Furthermore, the pH of the reaction medium was adjusted to 10 by adding 1 M ammonia solution by dropwise and the reaction was held at 50 °C. During the experiment, the suspension was mechanically stirred for 1 hour. MωOTS was collected by filtering and then washed with pure water for several times to remove unnecessary ions until the effluent had a pH value of about 7. Then, MωOTS was separated from the mother liquid phase by centrifugation. Then, the MωOTS was dried approximately 36 h at the room temperature. The dried adsorbent was heated with at 500 °C for 1 h to obtained biochar. The MBωOTS was stored for further experimental usage.

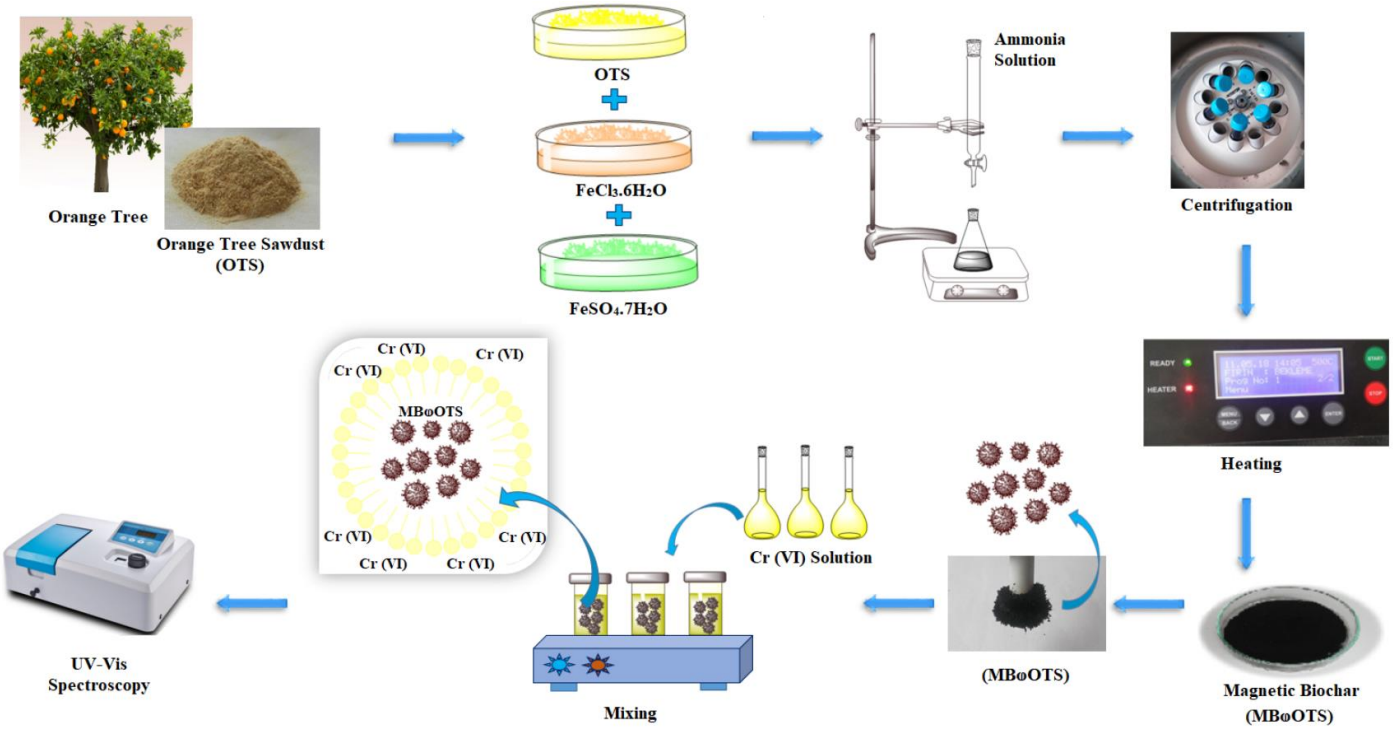

Figure 1. Preparation of MBωOTS from OTS.

2.3. Experimental Method

OTS and MBωOTS were tested as an adsorbent for the Cr (VI) removal. The batch equilibrium studies were conducted by adding a uniform quantity 0.1 g of the dried OTS and 0.05 g of the MBωOTS to 25 mL of the synthetic aqueous Cr (VI) solution having different initial concentrations (25–400 mg L^{-1}) in 100 mL flasks. The solutions were mixed well with a magnetic stirrer and maintained for a fixed time at 25 °C. To determine the adsorption capacity at various pHs, the pH of the Cr (VI) solution was adjusted with 0.1 M HCl or 0.1 M NaOH aqueous solutions to confirm the attainment of equilibrium. After the establishment of equilibrium, the residual concentration of the Cr (VI) in the filtrate was measured with a UV-Vis. Spectrophotometer.

2.4. Characterization of MBωOTS

The surface structure of MBωOTS was analysed by scanning electronic microscopy (SEM) (Figure 2.). As shown in Figure 2a., the typical SEM image indicates that a lot of iron nanoparticles uniformly dispersed on the surface of MBωOTS. The textural structure examination of MBωOTS particles can be observed from the SEM photographs. This figure reveals that the MBωOTS particles were mostly

irregular in shape and porous. Element distribution maps and general EDS analysis results of MBωOTS were given in Figure 2. (b, c, d, e, f). The distribution of the iron, oxygen, nitrogen and carbon in the MBωOTS was characterized by mapping as shown in Figure 2. (b, c, d, e), respectively. When the element distribution mapping is examined, it is seen that the synthesized iron is distributed homogeneously in the structure of adsorbent. EDX spectrum of the prepared MBωOTS is depicted in Figure 2f., which indicates the presence of iron, oxygen, nitrogen, and carbon. Table inset in Figure 2f. depicts the elemental analysis of the MBωOTS, indicating the wt% of iron, oxygen, carbon, and nitrogen as 49.20, 26.12, 9.94 and 0.17, respectively.

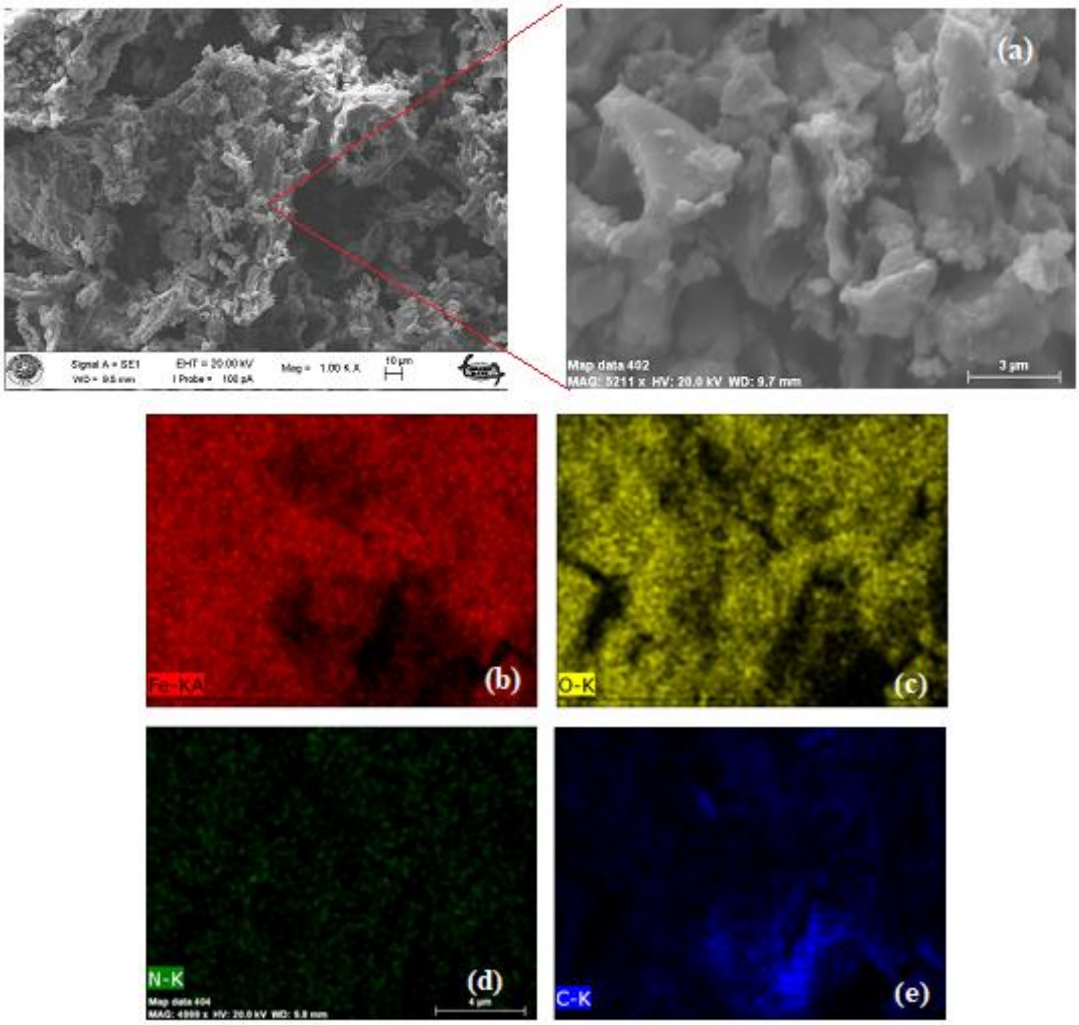

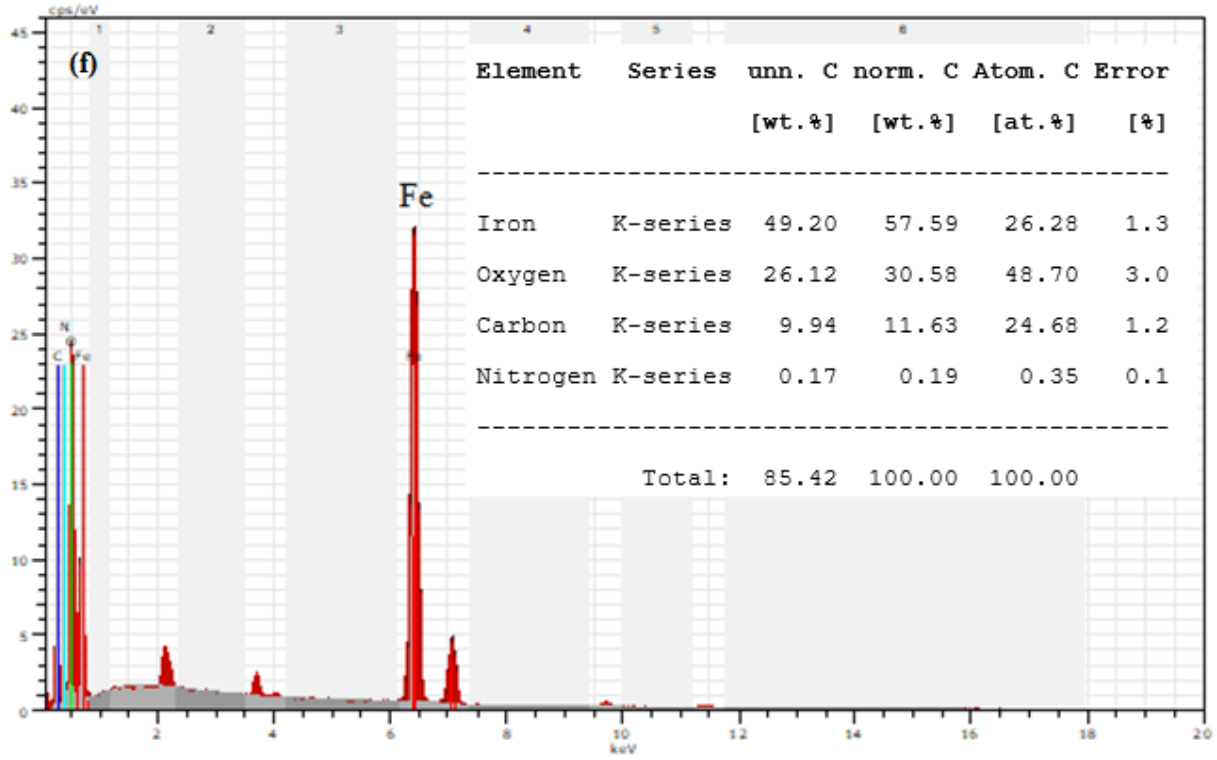

Figure 2. Typical SEM micrography of MB**ω**OTS **(a)**, the elemental mapping associated with iron, oxygen, nitrogen and carbon are depicted in **(b) (c) (d)** and **(e)**, respectively and EDX spectra of MB**ω**OTS **(f)**

The functional groups of OTS and MB**ω**OTS can be better understood from a FTIR study of the adsorbent. The spectra can, therefore, help in the interpretation of the functional groups accountable for adsorption. The FTIR spectrum of the raw OTS before adsorption (Figure 3.a) depicts a relatively broad peak at 3420 cm^{-1}, which is due to the H-bonded OH stretch, confirming the presence of a hydroxyl group. The band in the region of 2923 cm^{-1} was attributed to C–H stretching of alkane (Danish et al., 2018). The peak found within 1720-1620 cm^{-1} indicates the presence of carboxylic acid (C=O stretching vibration together with C–H stretching vibrations), which contains carboxyl and hydroxyl functional groups (Bardalai and Mahanta 2018). Aromatic C–O stretching vibrations of the lignin component and –C–O–C– stretching appearing at 1035 cm^{-1}. The MB**ω**OTS displays bands at 2597, 2163, 2044 and 1598 cm^{-1}(Figure 3.b). The band around 1598 cm^{-1} in MB**ω**OTS was assigned to ring vibration in a large aromatic skeleton or carbon-carbon double bonds generally found in activated carbon (Guo and Rockstraw, 2007; Liu et al. 2010). This band was attributed to the stretching vibration and the torsional vibration of Fe–O bonds in the tetrahedral sites and in the octahedral sites of Fe_3O_4 (Namduri and Nasrazadani. 2008; Liu et al. 2010; Reza and Ahmaruzzaman, 2015). Looking at the spectrum, it shows carboxylic acid, and hydroxyl groups showed a dominant role in the removal of Cr (VI) ions. Some clear shifts from the matrix of the adsorbents were seen after the adsorption of Cr (VI). This caused the decrease in the intensity of the band and changed the existing band to a narrow band spectrum. FTIR analysis of the adsorbents displayed that some bands shifted after Cr (VI) adsorption.

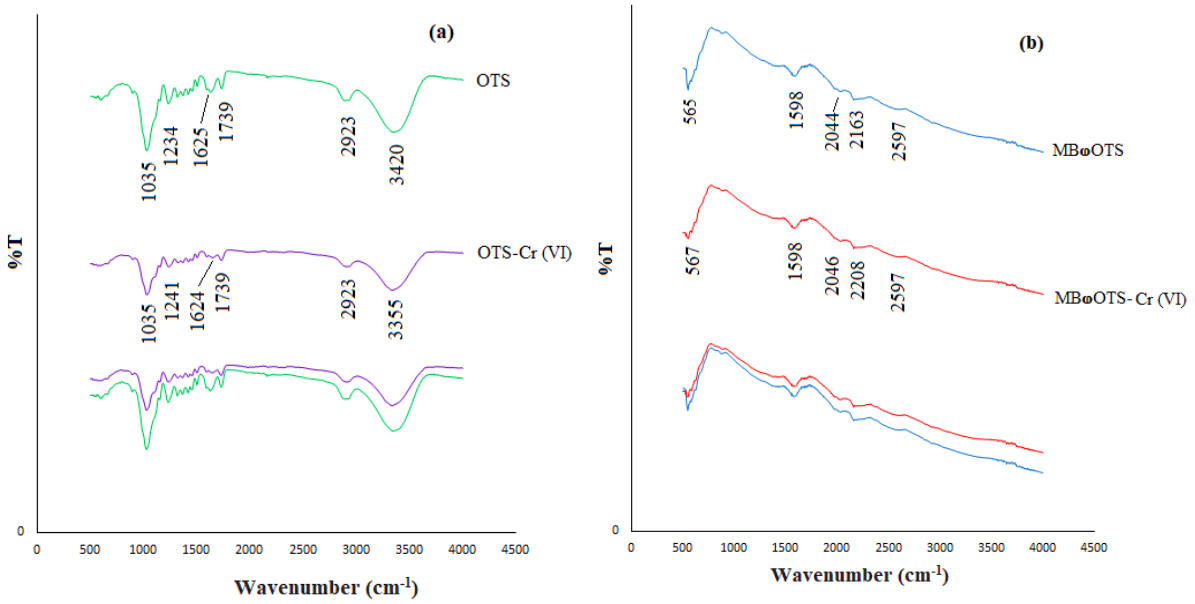

Figure 3. FTIR spectrum of OTS **(a)**, MBωOTS **(b)** before and after adsorption Cr (VI).

3. RESULTS AND DISCUSSION

3.1. Effect of Contact Time

The effect of contact time on the removal of Cr (VI) was showed in Figure 4. Contact time plays a significant role in the removal of Cr (VI). At first, the rise in adsorption is incredibly speedy as there are plenty of free sites for the adsorption to take place. The adsorption decreases at later stages until the equilibrium is reached because of the saturation of active sites. The quickest Cr (VI) uptake took place within the initial 30 min followed by slow uptake of the Cr (VI) for the next 180 min and eventually reached equilibrium after 180 min by using OTS and MBωOTS. The reason for this trend is that originally there's the accessibility of an oversized variety of vacant binding sites on the adsorbent surface promoting fast adsorption of Cr (VI). But, later on, the binding sites are being occupied gradually with time leading to the saturation of the adsorbent surface with the Cr (VI) molecules. Finally, once all the sites are occupied slowly, no subsequent adsorption takes place. The process then progressively decreases with time till it reaches the equilibrium due to the difficulty to access the remaining vacant adsorption sites.

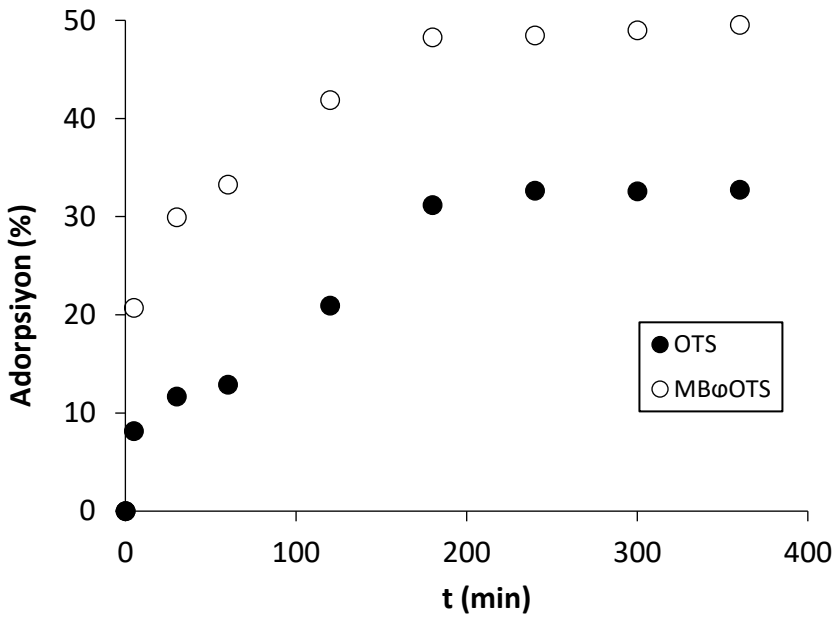

Figure 4. The effect of contact time on removal of Cr (VI) ions with **a)** OTS and **b)** MB**ω**OTS (Adsorption conditions: Cr (VI) concentration: 40 ppm, adsorbent amount: 0.1g, pH: 2, temperature: 25 ± 1 °C for OTS and Cr (VI) concentration: 40 ppm, adsorbent amount: 0.05g, pH: 2, temperature: 25 ± 1 °C for MB**ω**OTS.)

3.2. Effect of Solution pH

The relationship between the initial pH of the solution and Cr (VI) adsorption was investigated in pH studies. The influence of the initial aqueous pH solutions on Cr (VI) removal from the synthetic solutions by the OTS and MB**ω**OTS were investigated in a series of experiments for initial pH values of 1.5, 1.75, 2.0, 3.0, and 4.0 (Figure 5.). For the batch trails, pH was adjusted using small volume samples of 0.1 M HCl, and NaOH solutions. When the pH is lower then 1.8, the adsorption was decreased and it reached a maximum pH value at pH 1.9. When the pH of the solution is 2.0, the adsorption was also higher and this value was accepted as the maximum pH value for all experiments. It was observed that Cr (VI) residue on the adsorbent was lower at high pH values. Over pH 2.5, a slower Cr (VI) adsorption was observed.

Different mechanisms such as electrostatic interaction, ion exchange and chemical complexation are the mechanisms that may occur during adsorption. One of the mechanisms commonly proposed for the effect of pH on Cr (VI) adsorption is electrostatic interaction. It is important to have a proton abundance on the surface of the adsorbent for the rapid removal of Cr (VI). When the adsorbent surface is loaded with protons (positive surface), the electrostatic interaction takes place on the surface between Cr (VI) and the MB**ω**OTS. The increase of Cr (VI) adsorption at acidic pH should be due to the electrostatic attraction between positively charged groups of MB**ω**OTS and the $HCrO_4^-$ anion, which is the dominant species at low pH. The decrease of the adsorption with increasing pH could be due to the decrease of electrostatic attraction and to the competitiveness between the chromium species ($HCrO_4^-$ and CrO_4^{2-}) and OH^- ions in the solution phase for the adsorption on the active sites of the adsorbent. Cr (VI) may exist in the fluid stage in numerous anionic forms, such as chromate (CrO_4^{2-}), dichromate ($Cr_2O_7^{2-}$), or hydrogen chromate ($HCrO_4^-$), with full chromate concentrations and pH dictating which specific chromate species dominate. By lowering the pH of the solution, Cr (VI) adsorption increases to a certain pH, by creating more $HCrO_4^-$ at the expense of $Cr_2O_7^{2-}$. At slightly acidic pH, $HCrO_4^-$ is the most common sort of Cr (VI) species, but during Cr (VI) adsorption at acidic pH, $Cr_2O_7^{2-}$ is also president inside the adsorbent.

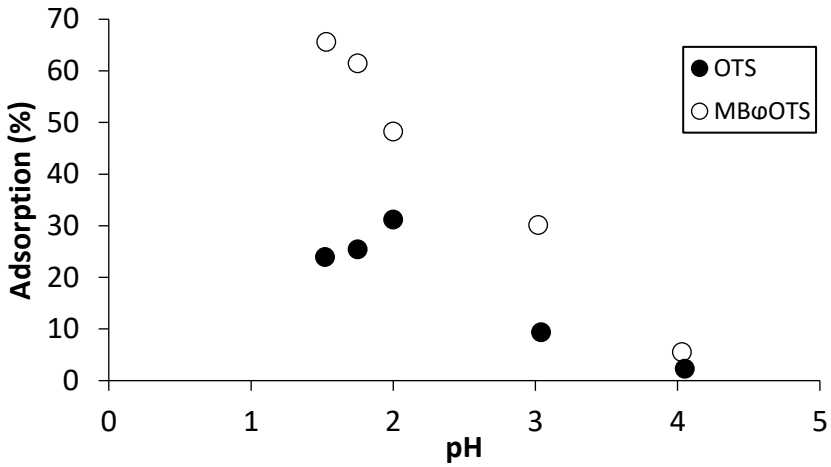

Figure 5. Effect of pH on adsorption of Cr (VI) ions with **a)** OTS and **b)** MB**ω**OTS (Adsorption conditions: Cr (VI) concentration: 40 ppm, adsorbent amount: 0.1g, contact time: 180 min, temperature: 25 ± 1 °C for OTS and Cr (VI) concentration: 40 ppm, adsorbent amount: 0.05g, contact time: 180 min, temperature: 25 ± 1 °C for MB**ω**OTS.)

3.3. Adsorption Isotherms

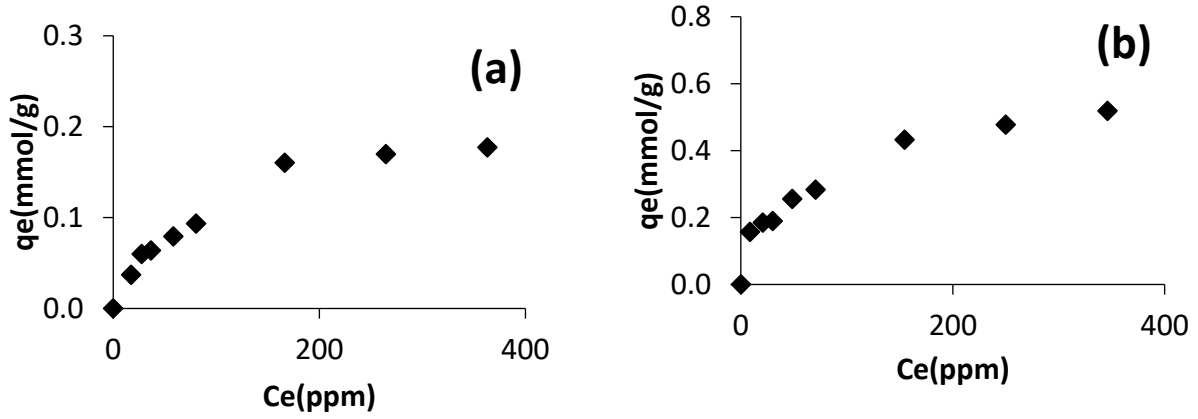

Figure 6. Adsorption isotherm **a)** OTS **b)** MB**ω**OTS. (Adsorption conditions: adsorbent amount: 0.1g, pH: 2; contact time: 180 min, temperature: 25 ± 1 °C for OTS and adsorbent amount: 0.05g, pH: 2; contact time: 180 min, temperature: 25 ± 1 °C for MB**ω**OTS.)

The adsorption isotherm models including Langmuir Eq. (1), Freundlich Eq. (2), Dubinin–Radushkevich (D-R) Eq. (3) and Scatchard Eq. (4) were used to fit and evaluate the equilibrium data corresponding to the adsorption of Cr (VI) on OTS and MB**ω**OTS (Figure 6.). The higher determination coefficients R^2>0.99 of the Langmuir equation suggest that the Langmuir equation can be used to fit the experimental adsorption data and to evaluate the maximum Cr (VI) adsorption capacity of the OTS and MB**ω**OTS. A_s and K_b were calculated from Eq. 1. and were given in Table 1. The maximum adsorption capacities of the Cr (VI) according to Langmuir isotherm model were 11.75 mg/g for OTS, 30.40 mg/g for MB**ω**OTS. The Langmuir isotherm model is generally applicable to monolayer adsorption on surfaces containing a certain number of similar sites. Information about the suitability of adsorption is also supported by R_L. If its value is between 0 and 1, it shows the suitability of the adsorption. R_L values are 0.697 for OTS; and 0.569 for MBωOTS. The Freundlich equation of K_f and n values were calculated from Eq. 2. n values were found to be 1.95 for OTS and 2.79 for MB**ω**OTS, indicating that the adsorption of these values was favourable from 1 to 10. Scatchard (Eq. 4.), related parameters are given in Table (1.), Qs values were 11.89 mg/g for OTS and 32.20 mg/g for MB**ω**OTS. D-R isotherm parameters were given in Table 1. E_{ad} values were found to be >8 kJ mol^{-1} (Eq. 3.). When the E_{ad} value is lower than 8 kJ mol^{-1}, the adsorption process is said to be predominant by physical adsorption. If E_{ad} is between 8

and 16 kJ mol^{-1}, the process is dominated by chemical ion exchange mechanisms and by chemical particle diffusion.

Table 1. Adsorption isotherm parameters for removal of Cr (VI)

MODEL	EQUATION	EQ	ADSORBENT	PARAMETERS FOR CR (VI)				REFERENCES
LANGMUIR	$\frac{C_e}{q_e} = \frac{C_e}{A_s} + \frac{1}{K_b A_s}$	(1)		A_S	K_B	R^2		(LANGMUIR, 1918)
			OTS	11.75	0.011	0.986		
			MBωOTS	30.36	0.019	0.989		
FREUNDLICH	$\ln q_e = \ln K_f + \frac{1}{n}\ln C_e$	(2)		K_F	N	R^2		(FREUNDLICH, 1906)
			OTS	0.51	1.95	0.966		
			MBωOTS	3.35	2.79	0.969		
D-R	$\text{IN } Q_E = \text{LN } Q_M - B\,E^2$	(3)		X_M **(x10^{-3})**	K	E	R^2	(DUBININ AND RADUSHKEVICH, 1947)
			OTS	0.52	0.007	8.77	0.977	
			MBωOTS	0.96	0.004	10.91	0.947	
SCATCHARD	$QE / C_E = Q_S K_S - Q_E K_S$	(4)		Q_S	K_S	R^2		(SCATCHARD, 1949)
			OTS	11.89	0.011	0.881		
			MBωOTS	32.20	0.014	0.966		

The results showed that the adsorption of Cr (VI) with OTS and MBωOTS takes place in a single-layer adsorption form. As shown in Table 2, the adsorption capacity of MBωOTS was compared with the other magnetic and biochar adsorbents. The capacity of MBωOTS is higher than others.

Table 2. Adsorption Capacity of OTS and MBωOTS Compared to The Other Published Low-Cost magnetic adsorbents for Cr (VI) Removal

Adsorbent material	Q_{max} (mg/g)	References
Magnetic porous carbonaceous (MPC) materials derived from tea waste	21.23	(Wen et al. 2017)
Magnetic biochar prepared with Astragalus membranaceus	23.85	(Shang et al. 2016)
Magnetic biochar prepared phoenix tree leaves Fe_3O_4@SiO_2-NH_2 magnetic particles	27.2	(Shi et al. (2018)
Magnetic biochar prepared Melia azedarach wood (MMABC)	25.27	(Zhang et al. 2018)
Chitosan combined with magnetic Loofah biochar (CMLB)	23.34	(Xiao et al. 2019)
MBωOTS	**30.36**	**This study**
OTS	**11.75**	**This study**

3.4. Effect of Adsorbent Dose

The impact of the adsorbent dosages on Cr (VI) removal was assessed for the adsorbent amount of 0.025, 0.05, 0.075, 0.10, 0.15 and 0.2g. It was noted that the adsorption percentage of Cr (VI) used for removal processes increases according to the amount of OTS and MBωOTS mass (Figure 7). This finding is justified by the high number of reactive available vacant sites forces the mass transfer of the Cr (VI) and the concentration gradient is high. This favours the transfer of the Cr (VI) to the external surface of adsorbent and increases on their removal percentage. As the adsorbents amount increases, there is an increase in the adsorption of Cr (VI) and as more the adsorbate concentration more is the adsorption exists on the surface of the adsorbents. The optimum dose was taken to be 0.1 g for OTS and 0.05 g for MBωOTS.

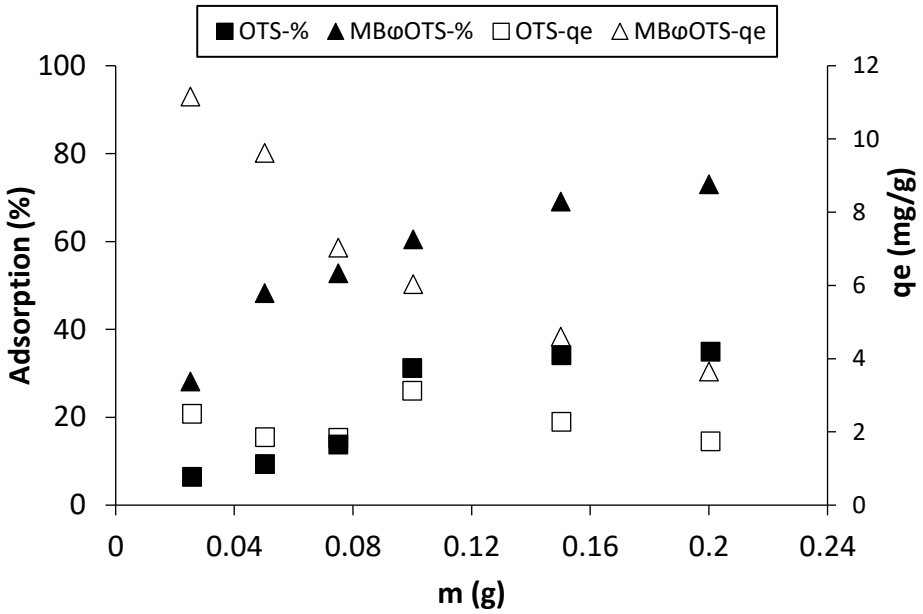

Figure 7. Effect of adsorbent amount on percentage removal and qe of Cr (VI) ions with **a)** OTS and **b)** MB**ω**OTS. (Adsorption conditions: Cr (VI) concentration: 40 ppm, pH: 2; contact time: 180 min, temperature: 25 ± 1 °C for OTS and Cr (VI) concentration: 40 ppm, pH: 2; contact time: 180 min, temperature: 25 ± 1 °C for MB**ω**OTS.)

3.5. Adsorption Kinetics

The pseudo first-order and pseudo second-order reaction equations were applied for the equilibrium system. Pseudo-first-order kinetic model and pseudo-second-order kinetic model for Cr (VI) on OTS and MB**ω**OTS have been demonstrated in Table 3. The pseudo-second-order kinetic model was used based on the following differential equation: where k_2 is the rate constant of pseudo-second-order adsorption (g mg^{-1} min^{-1}). The boundary condition q_t=0 at t=0 and the equation can be linearized as Eq. (5):

$$\frac{1}{q_t} = \frac{1}{k_2\ qe^2} + \frac{1}{q_e\, t} \qquad (5)$$

The pseudo-second-order kinetic model was found to agree between the experimental and calculated data, as indicated by the correlation coefficients higher than 0.99 obtained using this model.

Table 3. Kinetic parameters of Cr (VI) adsorption

		Pseudo First-order			Pseudo Second- order		
Adsorbent	qe_{exp}	k_1	q_e	R^2	k_2	q_e	R^2
OTS	3.29	0.016	3.40	0.954	0.0051	3.37	0.980
MB**ω**OTS	9.86	0.018	7.86	0.969	0.0048	10.38	0.995

4. CONCLUSION

In this research, a new magnetic adsorbent was prepared from OTS and effective conditions for Cr (VI) removal were determined by changing the initial Cr (VI) concentration, contact time, adsorbent amount and pH values. MB**ω**OTS was prepared from OTS and its property was intensively studied using SEM, EDX analyses. The novel produced MB**ω**OTS was tested for the removal of Cr (VI). MB**ω**OTS showed good selectivity for Cr (VI) removal. Langmuir, Freundlich, Scatchard and Dubinin-Radushkevich isotherms were tried and they were evaluated to determine the effectiveness of MB**ω**OTS. Langmuir isotherm model was preferred for the adsorption process (R^2 is 0.985). By applying the Langmuir model equation, the maximum Cr (VI) capacities of MB**ω**OTS and OTS were found to be 30.36 and 11.75 mg/g, respectively. MB**ω**OTS has a good adsorption capacity for removal Cr (VI) ions in the aqueous

solutions, which is compared with the raw OTS. The adsorption studies revealed that the optimum contact time for the equilibrium was found to be 180 min for MBϕOTS, OTS, respectively. An optimum pH value for the adsorption of Cr (VI) was found as 2.0. The produced adsorbent was generated from the natural sources that claim it is an environmental friendly adsorbent for the application of Cr (VI) removal from the polluted solution.

REFERENCES

Bardalai, M., and Mahanta, D. K., 2018, Characterisation of pyrolysis oil derived from teak tree saw dust and rice husk, *Journal of Engineering Science and Technology*, 13(1), 242–253.

Cao, W., Wang, Z., Ao, H. and Yuan, B., 2018, Removal of Cr(VI) by corn stalk based anion exchanger: the extent and rate of Cr(VI) reduction as side reaction, *Colloids and Surfaces A*,539, 424–432.

Chen, C., Zhu, K., Chen, K., Alsaedi, A. and Hayat, T., 2018, Synthesis of Ag nanoparticles decoration on magnetic carbonized polydopamine nanospheres for effective catalytic reduction of Cr (VI), *Journal of Colloid and Interface Science*, 526, 1–8.

Danish, M., Ahmad, T., Hashim, R., Said, N., Akhtar, M. N., Mohamad-Saleh, J., and Sulaiman, O., 2018, Comparison of surface properties of wood biomass activated carbons and their application against rhodamine B and methylene blue dye, *Surfaces and Interfaces*, 11, 1–13.

Dubinin, M. M., and Radushkevich, L. V., 1947, Evaluation of microporous materials with a new isotherm. In *Dokl. Akad. Nauk. SSSR*, 55, 331–334.

Freundlich, H. M. F., 1906, Over the biosorption in solution, *The Journal of Physical Chemistry*, 57, 385–471.

Gaikwad, M. S. and Balomajumder, C., 2017, Simultaneous rejection of fluoride and Cr (VI) from synthetic fluoride-Cr (VI) binary water system by polyamide flat sheet reverse osmosis membrane and prediction of membrane performance by CFSK and CFSD models, *Journal of Molecular Liquids*, 234, 194–200.

Gode, F., Atalay, E. D. and Pehlivan, E., 2008, Removal of Cr (VI) from aqueous solutions using modified red pine sawdust. *Journal of Hazardous Materials*, 152, 1201–1207.

Guo, Y., and Rockstraw, D. A., 2007, Physicochemical properties of carbons prepared from pecan shell by phosphoric acid activation. *Bioresource Technology*, *98*(8), 1513–1521.

Han, Y., Cao, X., Ouyang, X., Sohi, S. P. and Chen, J., 2016, Adsorption kinetics of magnetic biochar derived from peanut hull on removal of Cr (VI) from aqueous solution: Effects of production conditions and particle size, *Chemosphere*,145, 336–341.

Huang, Z., Dai, X., Huang, Z., Wang, T., Cui, L., Ye, J. and Wu, P., 2019, Simultaneous and efficient photocatalytic reduction of Cr(VI) and oxidation of trace sulfamethoxazole under LED light by rGO@Cu2O/ BiVO4 p-n heterojunction composite, *Chemosphere*, 221, 824–833.

Jia, Z., Shu, Y., Huang, R., Liu, J. and Liu, L., 2018, Enhanced reactivity of nZVI embedded into supermacroporous cryogels for highly efficient Cr(VI) and total Cr removal from aqueous solution, *Chemosphere*,199, 232–242.

Liu, Z., Zhang, F. S., and Sasai, R., 2010, Arsenate removal from water using Fe3O4-loaded activated carbon prepared from waste biomass, *Chemical Engineering Journal*, 160(1), 57–62.

Lyu, H., Tang, J., Huang, Y., Gai, L., Zeng, E. Y., Liber, K. and Gong, Y., 2017, Removal of hexavalent chromium from aqueous solutions by a novel biochar supported nanoscale iron sulfide composite, *Chemical Engineering Journal*, 322, 516–524.

Langmuir, I., 1918, The biosorption of gases on plane surfaces of glass, mica and platinum, *Journal of the American Chemical Society*, 40(9), 1361–1403.

Laqbaqbia, M., García-Payoa, M. C., Khayeta, M., El Kharrazc, J. and Chaouchb, M., 2019, Application of direct contact membrane distillation for textile wastewater treatment and fouling study, *Separation and Purification Technology*, 209, 815–825.

Lu, W., Li, J., Sheng, Y., Zhang, X., You, J. and Chen, L., 2017, One-pot synthesis of magnetic iron oxide nanoparticle-multiwalled carbon nanotube composites for enhanced removal of Cr(VI) from aqueous solution, *Journal of Colloid and Interface Science*, 505, 1134–1146.

Namduri, H., and Nasrazadani, S., 2008, Quantitative analysis of iron oxides using Fourier transform infrared spectrophotometry, *Corrosion Science*, *50*(9), 2493–2497.

Qian, L., Shang, X., Zhang, B., Zhang, W., Su, A., Chen, Y., Ouyang, D., Han, L., Yan, J. and Chen, M., 2019, Enhanced removal of Cr(VI) by silicon rich biochar-supported nanoscale zero-valent iron, *Chemosphere*, 215, 739–745.

Qian, L., Zhang, W., Yan, J., Han, L., Chen, Y., Ouyang, D. and Chen, M., 2017, Nanoscale zero-valent iron supported by biochars produced at different temperatures: Synthesis mechanism and effect on Cr(VI) removal, *Environmental Pollution*, 223, 153–160.

Rajapaksha, A. U., Alam, Md. S., Chen, N., Alessi, D. S., Igalavithana, A. D., Tsang, D. C.W. and Ok, Y. S., 2018, Removal of hexavalent chromium in aqueous solutions using biochar: Chemical and spectroscopic investigations, *Science of the Total Environment*, 625, 1567–1573.

Reza, R. A., and Ahmaruzzaman, M., 2015, A novel synthesis of Fe 2 O 3@ activated carbon composite and its exploitation for the elimination of carcinogenic textile dye from an aqueous phase, *RSC Advances*, *5*(14), 10575–10586.

Scatchard, G., 1949, The attractions of proteins for small molecules and ions, *Annals of the New York Academy of Sciences*, 51, 660–672.

Shukla, A., Zhang, Y.H., Dubey, P., Margrave, J.L. and Shukla, S. S., 2002, The role of sawdust in the removal of unwanted materials from water, *Journal of Hazardous Materials*, 137–152.

Shi, S., Yang, J., Liang, S., Li, M., Gan, Q., Xiao, K. and Hu, J., 2018, Enhanced Cr (VI) removal from acidic solutions using biochar modified by Fe3O4@ SiO2-NH2 particles, *Science of the Total Environment*, 628, 499-508.

Shan, C., Ma, Z. and Tong M., 2014, Efficient removal of trace antimony (III) through adsorption by hematite modified magnetic nanoparticles, *Journal of Hazardous Materials*, 268, 229–236.

Shang, J., Zong, M., Yu, Y., Kong, X., Du, Q. and Liao, Q., 2017, Removal of chromium (VI) from water using nanoscale zerovalent iron particles supported on herb-residue, *Biochar Journal of Environmental Management*, 197, 331–337.

Shang, J., Pi, J., Zong, M., Wang, Y., Li, W. and Liao, Q., 2016, Chromium removal using magnetic biochar derived from herb-residue, *Journal of the Taiwan Institute of Chemical Engineers*, 68, 289–294.

Son, E. B., Poo, K. M, Chang, J. S. and Chae, K. J., 2018, Heavy metal removal from aqueous solutions using engineered magnetic biochars derived from waste marine macro-algal biomass, *Science of the Total Environment*, 615, 161–168.

Tan, X., Liu, Y., Zeng, G., Wang, X., Hu, X., Gu, Y. and Yang, Z., 2018, Application of biochar for the removal of pollutants from aqueous Solutions, *Chemosphere*, 125 (2015) 70–85.

Vilardi, G., Ochando-Pulido, J. M., Verdone, N. and Stoller, M., 2018, On the removal of hexavalent chromium by olive stones coated by iron-based nanoparticles: Equilibrium study and chromium recovery, *Journal of Cleaner Production*, 190, 200–210.

Xiao, F., Cheng, J., Cao, W., Yang, C., Chen, J. and Luo, Z., 2019, Removal of heavy metals from aqueous solution using chitosan-combined magnetic biochars, *Journal of colloid and interface science*, 540, 579–584.

Xining, S., Jingjing, M., Zengqiang, Z. and Zhiyong, Z., 2015, Biosorption of hexavalent chromium from aqueous medium with the antibiotic residue, *Advance Journal of Food Science and Technology*, 7, 120–128.

Yap, M.W., Mubarak, N.M., Sahu, J.N. and Abdullah, E.C., 2017, Microwave induced synthesis of magnetic biochar from agricultural biomass for removal of lead and cadmium from wastewater, *Journal of Industrial and Engineering Chemistry*, 45, 287–295.

Zhang, S., Lyu, H., Tang, J., Song, B., Zhen, M. and Liu, X., 2019, A novel biochar supported CMC stabilized nano zero-valent iron composite for hexavalent chromium removal from water, *Chemosphere*, 217, 686–694.

Zhang, X., Lv, L., Qin, Y., Xu, M., Jia, X. and Chen, Z., 2018., Removal of aqueous Cr (VI) by a magnetic biochar derived from Melia azedarach wood, *Bioresource technology*, 256, 1–10.

Zakaria, Z.A., Suratman, M., Mohammed, N. and Ahmad, W.A., 2009, Chromium(VI) removal from aqueous solution by untreated rubber wood sawdust, *Desalination*, 244, 109–121.

WHO, 2011. Guidelines for Drinking-water Quality. world health organization, Geneva.

Wang, S., Tang, Y., Li, K., Mo, Y., Li , H. and Gu, Z., 2014, Combined performance of biochar sorption and magnetic separation processes for treatment of chromium-contained electroplating wastewater, *Bioresource Technology*, 174, 67–73.

Wen, T., Wang, J., Yu, S., Chen, Z., Hayat, T. and Wang, X., 2017, Magnetic porous carbonaceous material produced from tea waste for efficient removal of As (V), Cr (VI), humic acid, and dyes, *ACS Sustainable Chemistry & Engineering*, 5(5), 4371–4380.

Wei, D., Li, B., Huang, H., Luo, L., Zhang, J., Yang, Y., Guo J., Tang, L., Zeng G. and Zhou, Y., 2018, Biochar-based functional materials in the purification of agricultural wastewater: Fabrication, application and future research needs, *Chemosphere*, 197, 165–180.